POLITECNICO
MILANO 1863

SCUOLA DI INGEGNERIA INDUSTRIALE
E DELL'INFORMAZIONE

EXECUTIVE SUMMARY OF THE THESIS

Analysis of the effects of the aortic conduit's geometry and mechanical behavior on heart valve prosthesis' test bench characterization

TESI MAGISTRALE IN MATERIALS ENGINEERING AND NANOTECHNOLOGY AND BIOMEDICAL ENGINEERING– INGEGNERIA DEI MATERIALI E DELLE NANOTECNOLOGIE E INGEGNERIA BIOMEDICA

AUTHOR: ARIANNA CALLERA

ADVISOR: MARIA LAURA COSTANTINO, ROBERTO FRASSINE

ACADEMIC YEAR: 2021-2022

1 Introduction

Nowadays the prosthesis options for heart valves are several and widely differentiated. Regardless of the type, all valves are tested according to ISO 5840, that contains information on how to perform all pre-clinical and clinical tests. In particular for this work the in vitro pulsatile test will be considered. The Standard accurately describes the test parameters, like pressure, frequency, and cardiac output, to be used and the requirements that the prosthesis must pass [1]. The set-up description is, however, less precise and no indications are given on the geometry and mechanical properties that conduits and chambers must have. As a result, all tubes are often straight and rigid. This work will concern itself with the conduit downstream the aortic valve, simulating the aorta, and introduce first a more physiological geometry and then mechanical properties. For the geometry the Valsalva sinuses are introduced following the geometry found in literature. This addition is expected to introduce the formation of vortexes that are believed to aid the closure of the valve [2]. For mechanical properties we decided to focus on the compliance, considering a value of 1 mL/mmHg [3]; this should modify the fluid dynamic behavior downstream the valve.

2 Polymer Characterization

2.1 Materials and methods

In order to replicate the aorta's compliance, it was decided to use a flexible polymer and tailor its thickness to reach the desired characteristics. Since the geometry that we wanted to obtain was quite complex the chosen fabrication process was 3D printing. Starting form tensile strength and elongation at break the resin Elastic 50A from Formlabs (Formlabs Inc., Somerville, MA, USA) was selected. To have a complete material characterization different tests were performed.

Tests

Since no precise information on the material's nature was available, we decided to perform a swelling test to verify weather or not was crosslinked and if any water absorption would happen. Samples were put in contact with propanol, toluene and water and weighted at different time points.

In order to calculate the thickness needed for the desired compliance tensile tests were performed on a dynamometer to find the elastic modulus as a function of applied strain. Then the following equations were used to determine the thickness:

$$\Delta A = \frac{C}{l} * \Delta P$$

$$\Delta A = \pi * {r_0}^2 * \left[\left(1 + \frac{P_2 * r_0}{E_2 * t}\right)^2 - \left(1 + \frac{P_1 * r_0}{E_1 * t}\right)^2\right]$$

Since it was possible that 3D printing introduced a level of anisotropy, samples were printed along different directions and underwent tensile tests.

Since we are dealing with a polymeric material a series of stress relaxation experiments was performed to identify the linear viscoelasticity region.

To confirm that the calculated thickness would lead to the correct compliance a sample conduit was fabricated and used for a pressurization experiment.

To better characterize the material a creep experiment was performed on the dynamometer to characterize the viscoelastic transition.

To verify that the material would survive testing different cyclic experiments were performed; first at reduced frequency with the dynamometer and then at 1,2 and 5 Hz with a DMA apparatus.

The last test performed was an aging test to see if the material's properties would be altered with time. Samples were produced at the same time, divided between air contact and water submersion, and testes at different time points.

2.2 Results

From the swelling test no degradations showed, meaning that the material is crosslinked. We observed a 4.5% increase in weight in water, indicating water absorption.

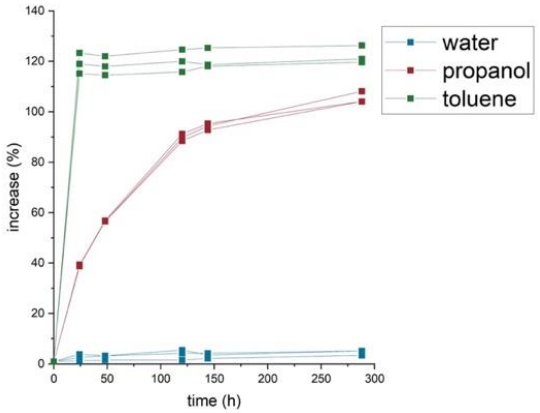

Figure 2.1: Percentage weight increase during swelling test

The tensile tests showed good repeatability and from the derived modulus function a thickness of 1.82 mm was calculated.

The isotropy test indicated that no difference is present in the slope of the curves for samples printed in different directions. A loss of strength was instead observed in those configurations that required a high number of supports to be placed in the test length.

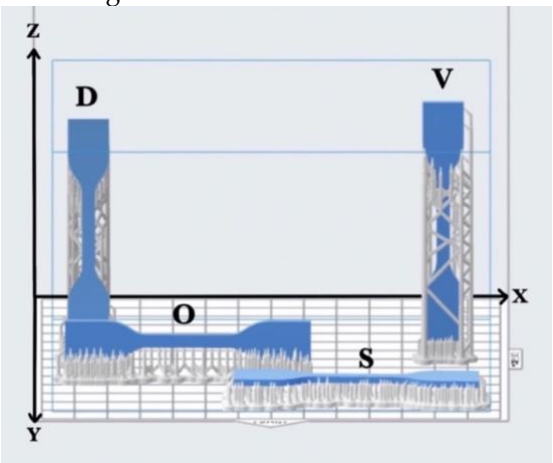

Figure 2.2: Different printing orientations with support placement

This test underlined the fundamental importance of a correct support placement to avoid strength losses.

From the stress relaxation experiments isochronous curves were derived. From these curves it was derived that the linear approximation is no longer valid after 1% strain.

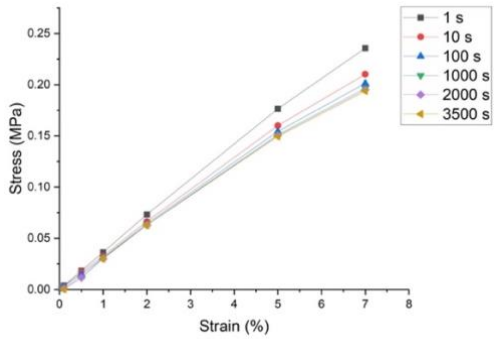

Figure 2.3: Isochronous curves derived from stress relaxation experiments

Due to isochronous curves overlapping it was also concluded that the viscoelastic transition happens in less than 100s.
The linearity results were confirmed in the pressurization test were the compliance stayed constant until 1% radial deformation and then increased following the decrease of elastic modulus. The compliance, in the physiological range of 80 to 120 mmHg, is within a 20% error of the target value.
From the creep test the only deductible information was that the viscoelastic transition was fast; the transition overlapped with the loading curve, so it was impossible to gather more precise information.
The material survived 350 cycles between 0 and 25% strain at reduced frequency; a 5% maximum stress reduction due to strain induced softening and a 0.008% residual deformation was observed indicating low plastic deformation. The material was deemed appropriate for cyclic tests as long as several cycles were given for conditioning before the start of recording. From the DMA tests we concluded that both conservative and dissipative modulus increase with frequency.

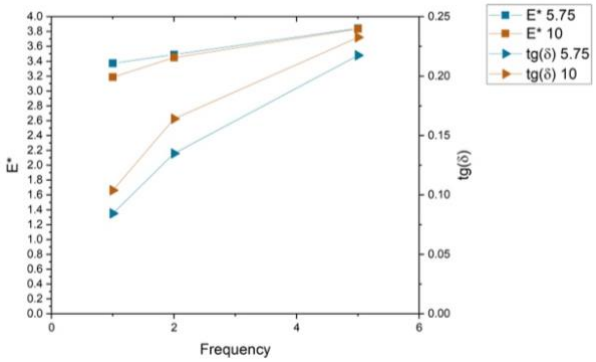

Figure 2.4: Complex modulus and tangent of δ resulting from DMA experiments

The aging tests showed that the material's rigidity increased with time in the air exposed samples, the effect was strongly reduced in the ones submerged with water. The material was UV crosslinked and likely some unreacted monomer was trapped in the structure, acting as a plasticizer. With time this monomer is released, and the material becomes more rigid.

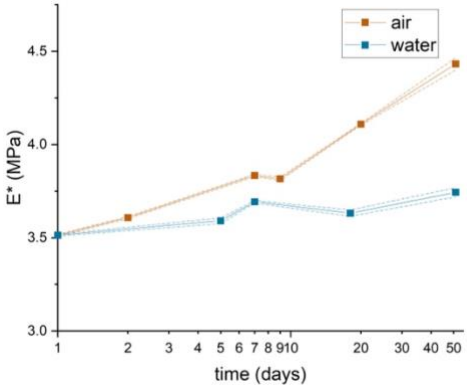

Figure 2.5: Aging results for the complex modulus

The water was absorbed by the submerged samples and acted as a plasticizer, compensating the monomer loss.

3 Valve Testing

3.1 Materials and methods

For the pulsatile tests an experimental test bench previously developed at Politecnico was used [4]; the portion of conduit downstream the aortic valve was modified.

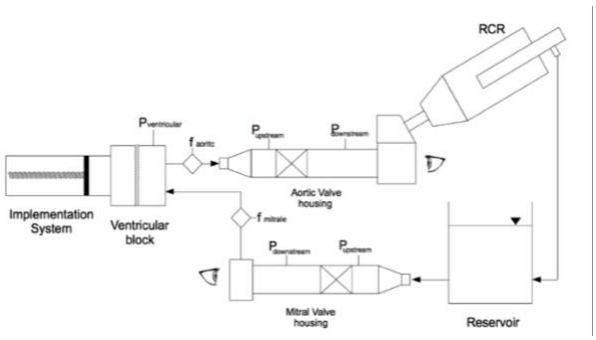

Figure 3.1: Schematic representation of the testing apparatus

Three set of tests were performed: with the rigid and straight conduit already present, with a rigid conduit with the geometry of the Valsalva sinuses and with a compliant conduit with the same geometry. The cross section of the Valsalva sinuses was modeled as an epitrochoid and the diameters

of the different sections were calculated from the given ratios considering a downstream diameter of 34mm, the same of the straight conduit [5].

Table 3.1: Geometrical ratios of the diameters shown in figure 3.2

D_b/D_0	D_a/D_0	L_a/D_0	L_b/D_0	R_{max}/D_0	R_{min}/D_0
1.55	1.25	1	0.34	0.82	0.64

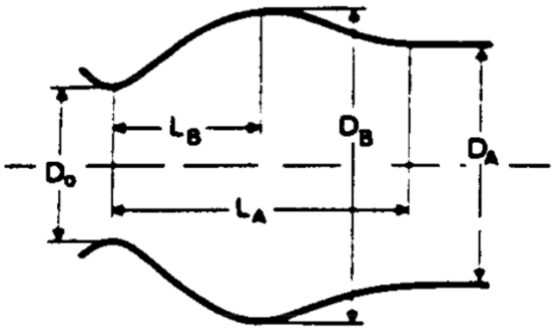

Figure 3.2: Schematic of the geometry of the aortic root with the different diameters

In order to analyze the effect of geometry and mechanical properties on different prosthesis each condition was tested with a bileaflet mechanical valve, a bovine stented biological valve, and a styrene block copolymer polymeric valve. The tests were performed in the physiological conditions indicated in the standard: 70 bpm, a systolic pressure of 120 mmHg, a diastolic pressure of 80 mmHg, and a cardiac output of 5 L/min. Pressure sensors were connected upstream and downstream the valve and two flow sensors, a 1" and a ½", were placed on the circuit. For each of the conditions average values were calculated for the following parameters: mean pressure difference during positive differential period, root mean square of forward flow, effective orifice area and regurgitation percentage.
A graphic analysis was also performed on flow, regurgitant flow, upstream and downstream pressure to analyze their behavior during a cycle.

3.2 Results

The introduction of Valsalva sinuses provoked an increment larger than 200% on the MPD of the mechanical valve while the other two showed a decrease. The mechanical valve is a bileaflet valve while the other two are trileaflet. The vortexes that form due to the sinuses interact well with the trileaflet geometry, aiding the opening of the valve, but not with the bileaflet, resulting in a larger pressure drop.
The introduction of compliance has a beneficial effect on the mechanical valve, reducing MPD, since in mitigates the vortexes directionality and smoothes out pressure differences. Due to the same effect, we expect MPD reductions for the other two valves; the unexpected behavior of the polymeric valve is correlated to a large positive differential pressure period in the rigid configuration that results in a lower average value.

Table 3.2: Results for MSPD in the different configurations

MSPD (mmHg)	Mechanical	Polymeric	Biological
Standard	24.0 ± 2.7	15.7 ± 3.2	21.8 ± 7.1
Valsalva sinuses rigid	89.6 ± 3.0	11.7 ± 2.3	17.0 ± 2.4
Valsalva sinuses compliant	26.5 ± 3.5	16.0 ± 1.4	13.6 ± 1.7

The forward flow is not much affected by the sinus's introduction, while decreases with the compliance. Since the stroke volume is kept constant by the volumetric pump, the differences are related to the increase of the positive differential pressure period in the compliant configuration.

Table 3.3: Results for Q_{RMS} in the different configurations

Q_{RMS} (ml/s)	Mechanical	Polymeric	Biological
Standard	12.0 ± 1.0	16.2 ± 1.2	15.8 ± 1.9
Valsalva sinuses rigid	16.6 ± 0.2	16.1 ± 0.8	14.6 ± 0.9
Valsalva sinuses compliant	14.2 ± 1.4	12.0 ± 1.4	12.6 ± 1.7

The EOA is directly proportional to Q_{RMS} and inversely proportional to the square root of MPD.

Its changes reflect the ones just treated. According to the Standard the EOA has to be at least 1.05 (cm^2) [1]; this value can be reached by the polymeric valve in two conditions and not completely in the other. It is evident how a manufacturer could perform the test in different configuration and simply present the more convenient result, eliminating the meaningful comparison between devices.

Table 3.4: Results for EOA in the different configurations

EOA (cm^2)	Mechanical	Polymeric	Biological
Standard	0.8 ± 0.1	1.4 ± 0.2	1.1 ± 0.2
Valsalva sinuses rigid	0.57 ± 0.01	1.6 ± 0.2	1.2 ± 0.1
Valsalva sinuses compliant	0.9 ± 0.1	1.0 ± 0.1	1.1 ± 0.2

The introduction of Valsalva sinuses provokes the formation of vortexes. This results in the reduction of regurgitation in the mechanical and polymeric valve. For the biological one instead the regurgitation is increased; this could be due to a high paravalvular leakage due to a mismatch of the support. When the compliant conduit is introduced, the regurgitation increases in all valves. This happens because the conduits expands and recoils following the pulsation of the pump, during recoil the fluid would physiologically be pushed into the coronaries but, since they are not present in the set up, it is pushed back towards the valve, increasing regurgitation. According to the standard the regurgitation has to be under 10%. [1]; of the shown valves only the polymeric valve seams to match the requirement. It should be considered that the tests have been performed with saline solution instead of blood. In presence of blood some coagulation would happen around the Dacron ring and reduce the paravalvular leakage in the mechanical and biological valve.

Table 3.5: Results for regurgitation % in the different configurations

Regurgitation %	Mechanical	Polymeric	Biological
Standard	14.5 ± 1.3	6.5 ± 0.2	12.6 ± 0.4
Valsalva sinuses rigid	8.6 ± 0.6	5.9 ± 0.2	14.3 ± 0.1
Valsalva sinuses compliant	19.8 ± 0.7	7.0 ± 0.2	17.6 ± 0.3

The introduction of Valsalva sinuses had no effect on the flow's plot while the compliance allowed the flow to pass quicker, making the peak higher; since the total flow was controlled by the volumetric pump and stayed constant and the peak became narrower.

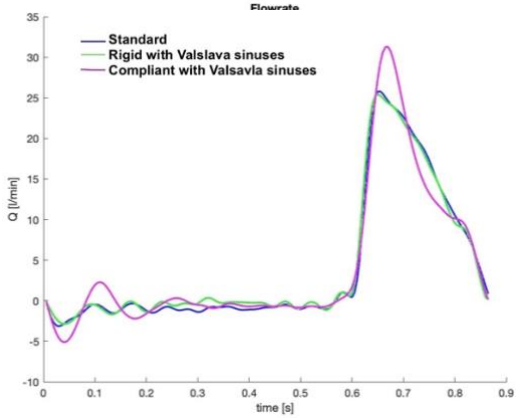

Figure 3.3: Flowrate behavior in a sample cycle for polymeric valve

The regurgitation flow decreases in presence of the Valsalva sinuses due to vortex formation; in particularly the closing volume is significantly reduced thanks to a faster closure. The introduction of compliance provokes a backflow with an increase of both closing and leakage volume.

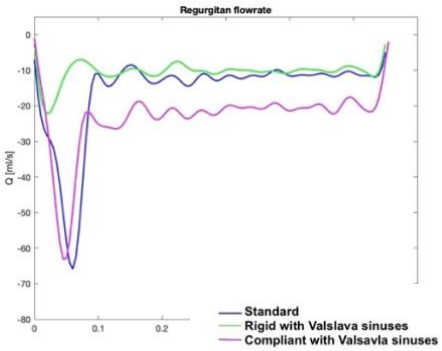

Figure 3.4: Regurgitant flow behavior in a sample cycle for mechanical valve

The upstream pressure increases in the configuration with Valsalva sinuses. This is due to the fact that when designing the conduit, in order to keep the diameter downstream the sinuses 34 mm like in the straight conduit, D_a in figure 3.2, the upstream diameter, D_0, ended up being 27 mm. This diameter reduction is the cause of the pressure increase. The compliance reduces the effect of the diameter reduction, and the pressure goes down.

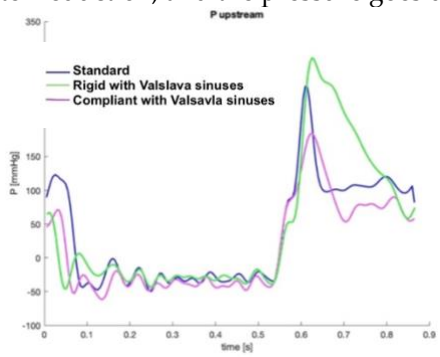

Figure 3.5: Upstream pressure behavior in a sample cycle for the mechanical valve

The downstream pressure is not affected by the presence of the Valsalva sinuses, but the compliant conduit provokes a delay in the peak since the sensor is placed downstream it.

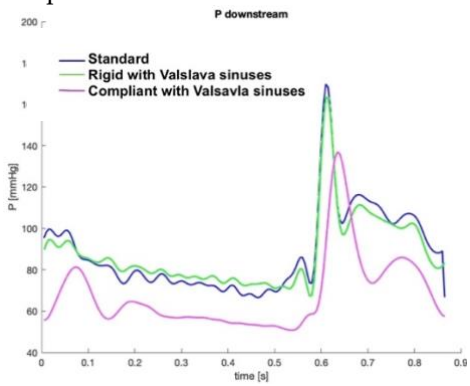

Figure 3.6: Downstream pressure behavior in a sample cycle for the biological valve

4 Conclusions

With the first part of this work, we proved the feasibility of fabricating an aortic phantom exploiting 3D printing and material's characterization. The second part, instead, showed how the geometrical and mechanical properties of the aortic conduit do have a significant influence on the performances of heart valve prosthesis during characterization. It emerges how the lack of a standardization for this conduit can easily lead to performances that cannot be compared to each other nor to a fixed minimum requirement.

5 References

[1] B. S. Institution, "Cardiovascular implants. Cardiac valve prostheses. Part 2, Surgically implanted heart valve substitutes.," 2021.

[2] M. S. Sacks and A. P. Yoganathan, "Heart valve function: A biomechanical perspective," *Philosophical Transactions of the Royal Society B: Biological Sciences*, vol. 362, no. 1484.

[3] R. M. Lang, B. P. Cholley, C. Korcarz, R. H. Marcus and S. G. Shroff, "Measurement of Regional Elastic Properties of the Human Aorta A New Application of Transesophageal Echocardiography With Automated Border Detection and Calibrated".

[4] F. De Gaetano, M. L. Costantino and S. Farè, "Design, manufacturing and in-vitro testing of an innovative biomorphic heart valve made of a new thermoplastic elastomeric biomaterial," Politecnico di Milano, 2017.

[5] H. Reul, A. Vahlbruch, M. Giersiepen, T. Schmitz-Rode, V. Hirtz and S. Effert, "The geometry of the aortic root in health, at valve disease and after valve replacement," *Journal of Biomechanics*, vol. 23, no. 2, 1990.